# Insights into the Mechanism of BN Generation via Boron Triazide Precursor: Theoretical Study

**ARTICLE** *in* THE JOURNAL OF PHYSICAL CHEMISTRY A · OCTOBER 2006

Impact Factor: 2.69 · DOI: 10.1021/jp062484c · Source: PubMed



**4 AUTHORS**, INCLUDING:

Fengyi Liu
Shaanxi Normal University
**25** PUBLICATIONS **293** CITATIONS
SEE PROFILE

Zheng Sun
Hebei Normal University
**63** PUBLICATIONS **587** CITATIONS
SEE PROFILE

# Insights into the Mechanism of BN Generation via Boron Triazide Precursor: Theoretical Study

**Fengyi Liu, Lingpeng Meng, Zheng Sun, and Shijun Zheng***

*Open Laboratory of Computational Quantum Chemistry, Hebei Normal University, Shijiazhuang 050016, P. R. China*

*Received: April 23, 2006; In Final Form: June 18, 2006*

Potential-energy surfaces for unimolecular decomposition of $B(N_3)_3$ have been studied to understand the possible mechanism for BN generation. The decomposition of $B(N_3)_3$ takes place on either the singlet and triplet surface, and both processes are high exothermic and obey sequential mechanisms. For the singlet reaction, the rate-determining step corresponds to cleavage of the first azide bond and linear $^1$NBNN instead of $^1$BN was suggested as the dominant product at room temperature. For the triplet surface, a fragment process from $^3BN_7$ to $^3BN_5$ is predicted to be the rate-determining step; once this barrier is counteracted, the subsequent decomposition processes could easily occur to form final product $^3$BN. In addition, the possible mechanism for generating BN film via $B(N_3)_3$ was discussed based on MC−SCF calculation results. These findings might be helpful in understanding the controllable decomposition of $B(N_3)_3$ as well as its application in generating BN films.

## Introduction

Boron triazide ($B(N_3)_3$) has been known for more than 50 years, since it was synthesized by Wiberg and Michaud in 1954.[1] Recently, the properties of $B(N_3)_3$ have attracted particular interest because it is suggested as a potential candidate for a high-energy density material (HEDM).[2−4] More importantly, Coombe and co-workers[5] demonstrated that decomposition of $B(N_3)_3$ leads to boron nitride (BN) and environmentally friendly nitrogen gases, which provides a novel way to generate nitrogen-rich BN thin film (thus far most BN films produced have been rich in boron not nitrogen[6]). Being isoelectronic with $C_2$, BN exhibits hexagonal (h-BN) and cubic (c-BN) structures in the solid phase; both forms have wide and important applications such as electrical insulators, crucibles, and reaction vessels, substrates for electronic devices, wear-resistant coatings, etc.[6−11] Compared to the current methods of producing BN film, which require the input of significant amounts of energy, generating BN via decomposition of highly energetic $B(N_3)_3$ does not require excessive energy input; therefore, problems associated with film damage caused by differential cooling or impact of high-energy species are avoided. Moreover, the BN film is expected to have much higher quality since the gaseous byproduct $N_2$ is easily eliminated and incorporation of unwanted species may be considerably mitigated.[12−14] Very recently, we reported a convenient method for generating $B(N_3)_3$ using the heterogeneous reaction of boron tribromide ($BBr_3$) with silver azide ($AgN_3$) powder at room temperature.[15] The experimental procedure could be easily carried out and higher purity product is expected when the amount of $BBr_3$ is well controlled. These findings might prompt further research on application of $B(N_3)_3$ as a precursor for BN thin film.

To date, the decomposition mechanism of $B(N_3)_3$ was far from known. Experimental attempts regarding the dissociation processes by which $B(N_3)_3$ reacts to form BN film have been reported by several laboratories. In 1995, Mulinux, Okin, and Coombe investigated the decomposition of $B(N_3)_3$ monitored by Fourier transform infrared (FTIR) and ultraviolet (UV) absorption spectroscopy.[5] Their results show gaseous $B(N_3)_3$ can be dissociated via either photolysis or thermolysis with final products BN and $N_2$. At room temperature $B(N_3)_3$ decomposes spontaneously to form hexagonal BN films, while this process occurs more rapidly and the final products display both hexagonal and cubic characteristics with addition of mild heating (50 °C) or upon irradiation with broadband UV light. The following equations were assumed in which both $BN_3$ and BN could be the final products

$$B(N_3)_3 \rightarrow BN_3 + 3N_2 \quad \text{(I)}$$

or

$$B(N_3)_3 \rightarrow BN + 4N_2 \quad \text{(II)}$$

These authors also reported the growth of boron nitride films via dissociation of $B(N_3)_3$ in excited $N_2$ stream.[12,13] They suggested that collisional energy transfer from $N_2$ ($A^3\Sigma_u^+$) should be responsible for dissociation of the molecule and subsequent deposition of BN films. In 1998, Gilbert and co-workers studied the photolytic decomposition mechanisms of $B(N_3)_3$ using low-temperature argon matrix and FTIR spectroscopy.[14] With the aid of CCSD(t)/6-311G* calculations, they identified formation of a linear intermediate NNBN instead of the trigonal $BN_3$ fragment expected from the photolytic cleavage processes known to occur in other covalent azides.[16,17] Thereafter, investigations on photolysis processes of related species including $BCl(N_3)_2$ and $BCl_2(N_3)$ using similar techniques were also reported by the same authors.[18−20] Except for the above-mentioned experimental achievements, no other information regarding dissociation of $B(N_3)_3$ is available. Therefore, a detailed study on the decomposition mechanism is highly desirable.

Besides the importance in interpreting the experimental results, research on decomposition of $B(N_3)_3$ has theoretical

* To whom correspondence should be addressed. Fax: 86-311-86269217. E-mail: sjzheng@mail.hebtu.edu.cn.

10.1021/jp062484c CCC: $33.50 
Published on Web 08/22/2006

significance since calculations of azides are always challenging.[21−24] It is known that a variety of processes might be involved in dissociation of azides, such as fragmentation, isomerization, and possible intersystem crossing (ISC) between the singlet and triplet surfaces, etc. Though the mechanism and reactivity of azide compounds, in particular photolysis and thermal decomposition of organic azides, have attracted much theoretical interest, heretofore the decomposition mechanism of molecules containing two or more azide groups has never been a subject of any previous reports. Open questions still remain in such systems, e.g., how these azide N−N bonds are ruptured, in a concerted or sequential manner? Which is the first process, fragmentation or isomerization? If these questions are well answered and a proper decomposition mechanism is determined, further theoretical and experimental research on multiple-azide compounds might be promoted consequentially.

In the present work, we attempt to characterize the full potential-energy surface (PES) for the unimolecular decomposition of $B(N_3)_3$ by density functional theory (DFT) calculation. Various possible fragmentation and isomerization processes were carefully mapped out, and all of the reactants, products, intermediates, and transition states on both the singlet and triplet surfaces were located. On the basis of these results, a reaction mechanism was suggested which might be helpful in understanding the dissociation process of $B(N_3)_3$ as well as its further application in BN film generating.

## Method of Calculation

As either thermolytic or photolytic processes are involved in the decomposition of $B(N_3)_3$, one can never expect a straightforward mechanism for it. Therefore, for all of the reactants, products, intermediates, and transition states in the reaction for both the singlet (close shell) and triplet (open shell) calculations were performed. The geometries of all compounds were optimized using the hybrid density functional B3LYP[25,26] with the 6-311+G(d) basis set which uses a polarization function and a diffuse function for each atom. Harmonic vibrational frequencies calculated at the same level were used for characterization of stationary points as a minimum or a saddle point and for zero-point energy (ZPE) corrections. Transition states were subjected to intrinsic reaction coordinate (IRC)[27] calculations to confirm the connection between reactants, intermediates, and decomposition products.

To obtain comprehensive reaction schemes, energies of stationary points were calculated at three levels of theory. The thermal enthalpies and Gibbs free energies (at 298.15 K and 1 atm) at the B3LYP/6-311+G(d) level were obtained for all reactants, intermediates, products, and transition states to evaluate the thermodynamic properties of the reaction. In addition, based on the B3LYP/6-311+G(d)-optimized geometries, calculations at the CCSD(T)[28]/cc-PVDZ[29] and B3LYP/6-311++G(3df) level were performed to obtain the relative energies for these species.

Moreover, to find the intersystem crossing between the singlet and triplet surface in the decomposition processes, the multiconfiguration SCF (MC-SCF)[30] method and 6-31G(d) basis sets were employed. In MC-SCF calculation, six electrons and five orbitals were including in the active space.

All quantum calculations were performed with the Gaussian 98 program.[31]

## Results and Discussion

On the whole, results of our calculation indicate that in either the singlet or the triplet processes unimolecular reaction of $B(N_3)_3$ follows a four-step mechanism:[5] (1) $B(N_3)_3 \rightarrow BN_7 + N_2$; (2) $BN_7 \rightarrow BN_5 + N_2$; (3) $BN_5 \rightarrow BN_3 + N_2$; (4) $BN_3 \rightarrow BN + N_2$. At each step a $N_2$ molecule was eliminated from $BN_x$ ($x = 9, 7, 5, 3$) due to cleavage of the azide N−N bond (or B−N bond in some cases) followed by rearrangement of the remaining $BN_{x-2}$ moieties. In other words, the title reaction, $B(N_3)_3 \rightarrow BN + 4N_2$, takes place in a sequential manner instead of a concerted one. Since the energy resulting from $N_2$ formation is released stepwise, though the total reaction is very exothermic, accumulation of a large energy that might lead to an explosion could be avoided. This finding is consistent with the previous experimental observations[5] that decomposition of $B(N_3)_3$ occurs mildly at room temperature, in contrast to most covalent azides that explode uncontrollably.

The geometries of the reactants, products, potential intermediates, and transition states located on the singlet reaction surface are shown in Figure 1, and all geometries on the triplet surface are shown in Figure 2. Their zero-point vibrational energies (ZPE), relative values of thermal enthalpies ($\Delta H°$), and Gibbs free energies ($\Delta G°$) as well as the relative energies calculated at the B3LYP/6-311++G(3df) (denoted as $\Delta E_{B3LYP}$) and CCSD(t)/cc-PVDZ ($\Delta E_{CCSD}$) levels of theory are summarized in Table 1 for the singlet state and Table 2 for the triplet state.

From Tables 1 and 2 it is seen that in some cases the CCSD(t)/cc-PVDZ calculation fails to give proper barrier heights. For instance, both the B3LYP/6-311++G(3df) energies and the IRC results at the B3LYP/6-311+G(d) level (Supporting Information, Table S4, reaction 2) indicate dissociation of $^1NB(N_3)_2$ has a low barrier, while the CCSD(t) results suggest this process to be barrierless because $^1NB(N_3)_2$ lies above its dissociation transition state $^1$TS2a by 1.7 kcal·mol$^{-1}$ (Table 1). That is, the CCSD(t)/cc-PVDZ calculation underestimates the barrier height of this reaction. It is understandable because these disagreements generally result from the changes in geometries from B3LYP/6-311+G(d) to CCSD(t)/cc-PVDZ. Though ideally the same method should be used in both geometry optimization and energy calculation and it is foreseeable that the CCSD(t)-optimized geometries are superior to the B3LYP results, CCSD(t) optimization is unfeasible in such systematic calculations. Luckily, the changes in geometry do not evidently affect the relative importance of various product channels. In addition, it is also found that the relative energies calculated at the B3LYP/6-311++G(3df) level are reasonable. Therefore, although disagreements do exist, the results of CCSD(t)/cc-PVDZ//B3LYP/6-311+G(d) are reliable with the aid of B3LYP/6-311++G(3df) energy prediction.

The detailed reaction mechanisms for the singlet and triplet process are discussed below.

**1. Singlet Reaction Mechanism.** The singlet unimolecular reaction of $B(N_3)_3$, with final products $^1$BN and ground state $^1N_2$, is denoted as $^1B(N_3)_3 \rightarrow {}^1BN + 4\,{}^1N_2$. This process is very complicated and involves 25 stationary points consisting of the reactant, products, intermediates, and transition states. Fourteen elementary reactions in this process, which were classified into four steps, are shown in Table 3.

The first step of the singlet reaction corresponds to cleavage of the first azide bond in $^1B(N_3)_3$ via $^1$TS1, leading to $^1NB(N_3)_2$ and $N_2$ (reaction 1). The geometry of $^1B(N_3)_3$ has been reported previously by several groups at the Hartree−Fock[5] and DFT[15] levels of theory. All results suggest a planar molecular with $C_{3h}$ symmetry in which the central boron atom is surrounded by three equivalent azide arms. Due to the existence of the electron-deficient $\Pi_{10}^9$ delocalization, the azide bonds in $^1B(N_3)_3$ are hard to rupture. From Figure 1 it can be seen

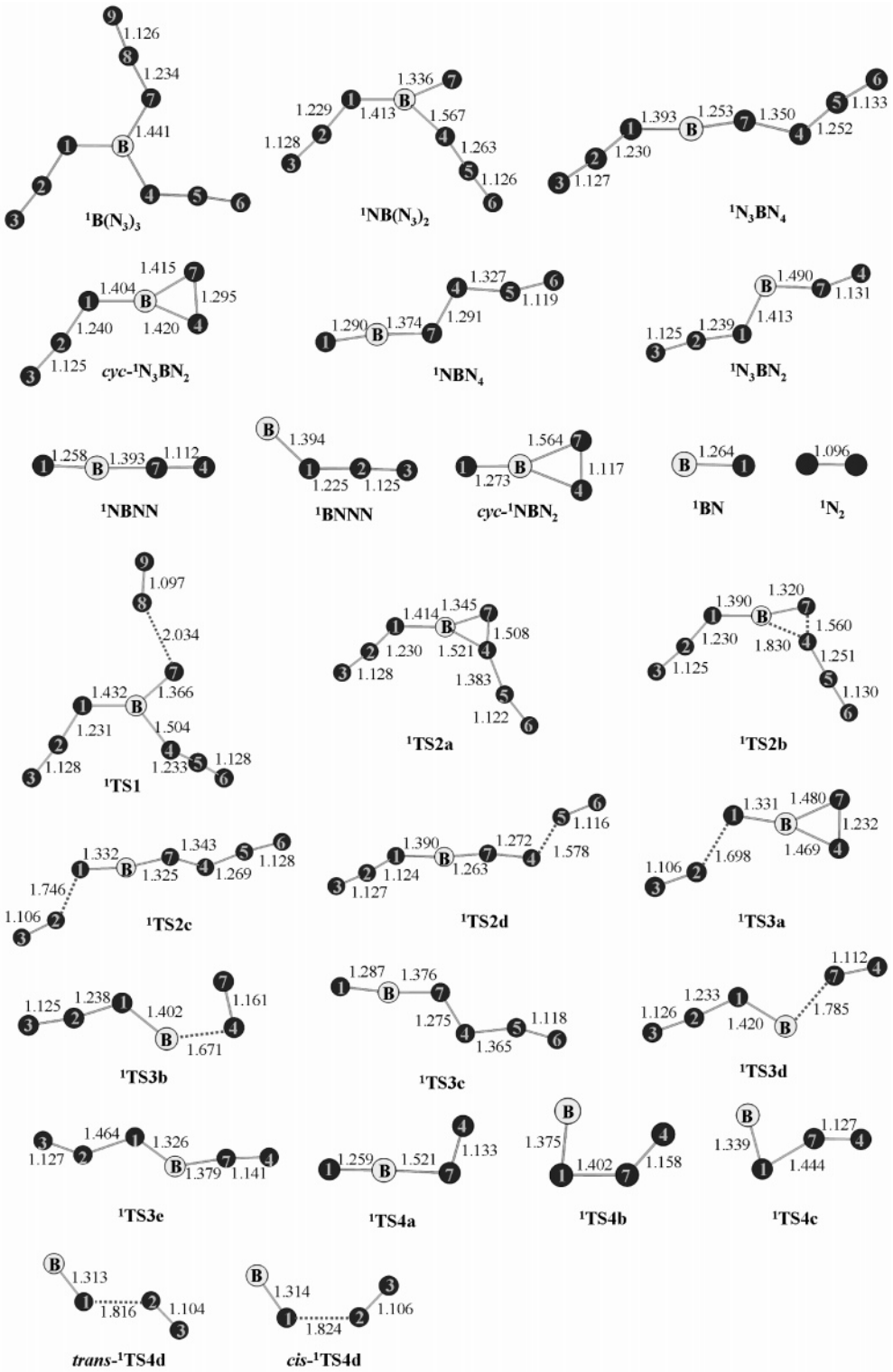


**Figure 1.** B3LYP/6-311+G(d)-optimized geometries of various species involved in the $^1B(N_3)_3 \rightarrow {}^1BN + 4\,^1N_2$ reaction. Bond distances are in angstroms.

that before one of the three azide bonds is ruptured, the breaking N7−N8 bond elongates significantly; meanwhile, the neighbor N4−N5−N6 azide group rotates out of the molecular plane. As a result, in transition state $^1$TS1 the planar geometry of $^1B(N_3)_3$ is totally destroyed, leading to a high barrier (46.6 kcal·mol$^{-1}$) for this process. Finally, N8N9 move away to form $N_2$ with products $^1NB(N_3)_2$ and $N_2$ being 41.8 kcal·mol$^{-1}$ less stable than the reactant, which indicates the initial step of $^1B(N_3)_3$ decomposition is very endothermic. The reaction path for this process is illustrated in Figure 3.

The remaining $^1NB(N_3)_2$ molecule could decompose to form $^1BN_5$ or isomerize to an open-chain conformer, $^1N_3BN_4$. Correspondingly,$^1N_3BN_4$ also has the possibility to take part in further decomposition process. These reactions are summarized in reactions 2−5 in Table 3 and classified as the second step of the total reaction.

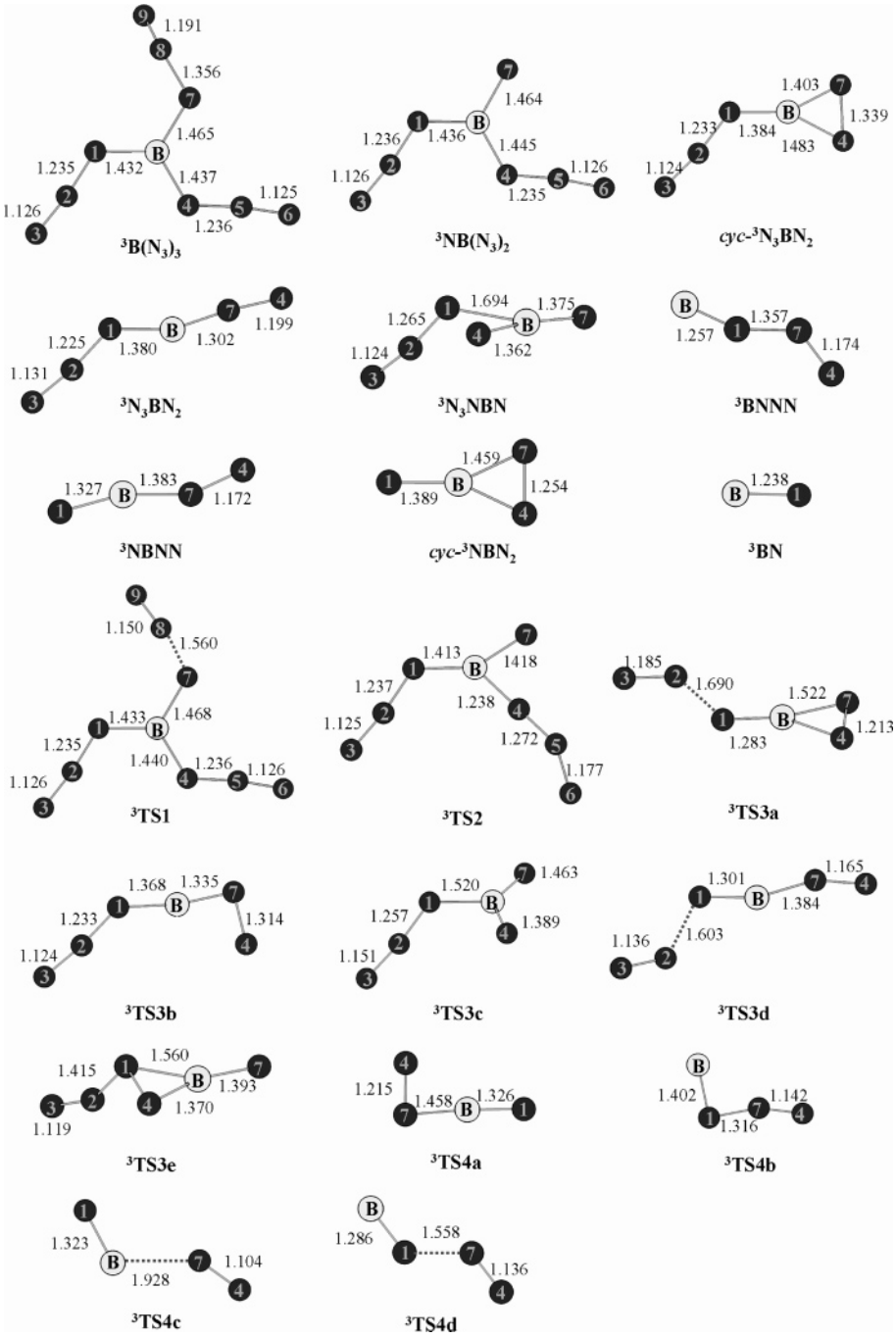


**Figure 2.** B3LYP/6-311+G(d)-optimized geometries of various species involved in the $^3B(N_3)_3 \rightarrow {}^3BN + 4\,^1N_2$ reaction. Bond distances are in angstroms.

*$^1NB(N_3)_2 \rightarrow$ cyc-$^1N_3BN_2 + {}^1N_2$ (Reaction 2).* $^1NB(N_3)_2$ has two azide groups, so theoretically two decomposition channels via cleavage of the in-plane N1−N2 or out-of-plane N4−N5 bond should be expected. However, the transition state corresponding to cleavage of the N1−N2 bond failed to be located in our calculation. It is understandable since the existence of a delocalized $\pi$ effect among the molecular plane stabilizes the in-plane N1−N2 bond and makes it more difficult to be ruptured. The found dissociation channel via $^1$TS2a resulting from cleavage of the N4−N5 bond yields *cyc*-$^1N_3BN_2$ and $N_2$. In $^1$TS2a a three-membered ring B−N4−N7 is formed and then carried over in the product *cyc*-$^1N_3BN_2$. Compared with reaction 1, the decomposition process of $^1NB(N_3)_2$ has a very earlier barrier on its reaction path (reaction 2, Table S4), the barrier height at the B3LYP/6-311++G(3df) level is predicted to be 1.3 kcal·mol$^{-1}$ (the CCSD(t)/cc-PVDZ calculation underestimates the barrier height again), and the products are over 65.0 kcal·mol$^{-1}$ more stable than the reactant. These facts suggest $^1NB(N_3)_2$ is thermodynamically less stable and tends to instantly decompose into $^1BN_5$ and $N_2$.

*$^1NB(N_3)_2 \rightarrow {}^1N_3BN_4$ (Reaction 3).* Besides the above-mentioned decomposition process, $^1NB(N_3)_2$ can also rearrange to straight-chain isomer $^1N_3BN_4$ in which N4−N5−N6 migrates from the B to N7 atom via a three-membered ring transition structure $^1$TS2b. The isomerization channel should be competitive with the decomposition process because of its low barrier height of 1.4 kcal·mol$^{-1}$. The product $^1N_3BN_4$, less stable than $^1NB(N_3)_2$ by only 1.8 kcal·mol$^{-1}$, has two azide groups, the N1−N2−N3 linked to B and the N4−N5−N6 linked to the

**TABLE 1: Changes of Enthalpies, Gibbs Free Energies, and Electronic Energies Calculated at Various Levels of Theory and Zero-Point Energies (ZPE, in kcal·mol$^{-1}$) for the $^1B(N_3)_3 \rightarrow {}^1BN + 4\,^1N_2$ Reaction**

| | B3LYP/6-311+G(d) | | | | |
|---|---|---|---|---|---|
| species | ZPE | $\Delta H°$ | $\Delta G°$ | $\Delta E_{B3LYP}$ | $\Delta E_{CCSD(t)}$ |
| $^1B(N_3)_3$ | 28.4 | 0.0 | 0.0 | 0.0 | 0.0 |
| $^1NB(N_3)_2 + N_2$ | 20.5 | 37.6 | 25.8 | 42.1 | 41.8 |
| $^1N_3BN_4 + N_2$ | 21.1 | 22.5 | 10.1 | 26.1 | 43.6 |
| *cyc*-$^1N_3BN_2 + 2N_2$ | 15.4 | −30.5 | −52.0 | −23.6 | −35.3 |
| $^1NBN_4 + 2N_2$ | 13.3 | 34.6 | 12.4 | 44.5 | 35.1 |
| $^1N_3BN_2 + 2N_2$ | 13.9 | −6.5 | −34.5 | 1.0 | −15.4 |
| $^1NBNN + 3N_2$ | 9.1 | −57.7 | −88.9 | −47.9 | −68.0 |
| $^1BNNN + 3N_2$ | 8.7 | −24.3 | −56.2 | −15.6 | −34.4 |
| *cyc*-$^1NBN_2 + 3N_2$ | 7.7 | −29.0 | −61.4 | −17.5 | −39.4 |
| $^1BN + 4N_2$ | 2.5 | 4.5 | −36.3 | 17.4 | −27.2 |
| $^1N_2$ | 3.5 | | | | |
| $^1$TS1 | 25.0 | 45.3 | 42.3 | 49.5 | 46.6 |
| $^1$TS2a + $N_2$ | 19.4 | 37.6 | 26.2 | 43.4 | 40.1 |
| $^1$TS2b + $N_2$ | 20.0 | 38.9 | 27.3 | 44.3 | 43.2 |
| $^1$TS2c + $N_2$ | 18.4 | 49.1 | 36.7 | 57.6 | 56.7 |
| $^1$TS2d + $N_2$ | 18.9 | 32.7 | 20.1 | 39.1 | 42.6 |
| $^1$TS3a + $2N_2$ | 12.8 | −10.2 | −32.4 | 0.5 | −12.3 |
| $^1$TS3b + $2N_2$ | 13.3 | 7.7 | −14.1 | 16.3 | 0.9 |
| $^1$TS3c + $2N_2$ | 12.7 | 33.2 | 11.4 | 44.0 | 35.0 |
| $^1$TS3d + $2N_2$ | 13.3 | −12.6 | −34.8 | −3.8 | −19.1 |
| $^1$TS3e + $2N_2$ | 12.7 | −3.6 | −25.7 | 6.6 | 1.3 |
| $^1$TS4a + $3N_2$ | 7.2 | −18.6 | −51.0 | −6.5 | −27.3 |
| $^1$TS4b + $3N_2$ | 7.2 | 4.0 | −27.4 | 15.3 | −6.8 |
| $^1$TS4c + $3N_2$ | 7.2 | −1.4 | −33.1 | 9.7 | −7.6 |
| *cis*-$^1$TS4d + $3N_2$ | 5.9 | 15.8 | −18.2 | 28.5 | -14.7 |
| *trans*-$^1$TS4d + $3N_2$ | 5.9 | 15.5 | −18.3 | 32.6 | −15.9 |

**TABLE 2: Changes of Enthalpies, Gibbs Free Energies, and Electronic Energies Calculated at Various Levels of Theory and Zero-Point Energies (ZPE, in kcal·mol$^{-1}$) for the $^3B(N_3)_3 \rightarrow {}^3BN + 4\,^1N_2$ Reaction**

| | B3LYP/6-311+G(d) | | | | |
|---|---|---|---|---|---|
| species | ZPE | $\Delta H°$ | $\Delta G°$ | $\Delta E_{B3LYP}$ | $\Delta E_{CCSD(t)}$ |
| $^3B(N_3)_3$ | 26.1 | 0.0 | 0.0 | 0.0 | 0.0 |
| $^3NB(N_3)_2 + N_2$ | 20.8 | −34.1 | −45.7 | −29.5 | −37.6 |
| *cyc*-$^3N_3BN_2 + 2N_2$ | 14.0 | −52.7 | −75.1 | −45.6 | −52.2 |
| $^3N_3BN_2 + 2N_2$ | 14.0 | −79.3 | −101.8 | −72.4 | −72.4 |
| $^3N_3NBN + 2N_2$ | 12.4 | −9.1 | −31.8 | 0.5 | −7.5 |
| $^3NBNN + 3N_2$ | 7.3 | −82.1 | −114.6 | −71.0 | −84.8 |
| $^3BNNN + 3N_2$ | 7.6 | −53.7 | −86.4 | −43.4 | −59.8 |
| *cyc*-$^3NBN_2 + 3N_2$ | 7.4 | −74.5 | −106.2 | −62.9 | −80.2 |
| $^3BN + 4N_2$ | 2.7 | −43.4 | −84.3 | −32.2 | −81.4 |
| $^3$TS1 | 24.9 | −2.8 | −5.1 | 1.3 | 0.3 |
| $^3$TS2 + $N_2$ | 18.7 | 13.8 | 2.0 | 20.6 | 23.0 |
| $^3$TS3a + $2N_2$ | 11.3 | −62.3 | −72.3 | −37.6 | −44.7 |
| $^3$TS3b + $2N_2$ | 13.3 | −8.8 | −17.8 | −43.0 | −47.9 |
| $^3$TS3c + $2N_2$ | 12.5 | −93.4 | −18.6 | 16.1 | 5.4 |
| $^3$TS3d + $2N_2$ | 11.6 | −62.0 | −29.6 | −37.3 | −57.3 |
| $^3$TS3e + $2N_2$ | 11.4 | 1065.7 | 1042.6 | 3.8 | −5.0 |
| $^3$TS4a + $3N_2$ | 6.9 | −66.5 | −98.7 | −54.4 | −71.8 |
| $^3$TS4b + $3N_2$ | 7.3 | −27.5 | −59.3 | −16.6 | −34.1 |
| $^3$TS4c + $3N_2$ | 6.3 | −71.2 | −104.8 | −19.8 | −82.6 |
| $^3$TS4d + $3N_2$ | 6.5 | −54.0 | −86.8 | −41.9 | −59.6 |

N7 atom. Consequently, the cleavage of either N1−N2 or N4−N5 bond might be involved in further fragmentation processes.

*$^1N_3BN_4 \rightarrow {}^1NBN_4 + {}^1N_2$ (Reaction 4).* This reaction via $^1$TS2c is similar to those in other azide compounds,[32,33] where cleavage of the N1−N2 bond is responsible for formation of $^1NBN_4$. The decomposition product $^1NBN_4$ is slightly more stable than the reactant by 8.5 kcal·mol$^{-1}$. However, it is less important because its barrier height of 13.1 kcal·mol$^{-1}$ is still higher than that in the following reaction 5.

*$^1N_3BN_4 \rightarrow {}^1N_3BN_2 + {}^1N_2$ (Reaction 5).* In this process cleavage of the N4−N5 bond results in formation of a new isomer of $BN_5$, $^1N_3BN_2$, which is far more stable than $^1NBN_4$ but still less stable than *cyc*-$^1N_3BN_2$. Again, CCSD(t)/cc-PVDZ gives an improper barrier height of −1.0 kcal·mol$^{-1}$; considering the low barrier predicted by B3LYP/6-311++G(3df) calculation, $^1N_3BN_4$ decomposing via $^1$TS2d is energetically more favorable than reaction 4.

Overall, both two isomers of $^1BN_7$, $^1NB(N_3)_2$, and $^1N_3BN_4$, are unstable and easily decompose into three isomers of $^1BN_5$. Among the above-mentioned reaction channels, reaction 2 ($^1NB(N_3)_2 \rightarrow$ *cyc*-$^1N_3BN_2 + {}^1N_2$) via $^1$TS2a is thermodynamically preferred, but other channels should not be neglected.

The third step of the total reaction corresponds to decomposition of $^1BN_5$. Each of the three isomers of $BN_5$, *cyc*-$^1N_3BN_2$, $^1NBN_4$, and $^1N_3BN_2$, will take part in further decomposition processes. As a result, there are five reactions (reaction 6−10,

**TABLE 3: The Reactions Involved in the Singlet Decomposition Pathway of $^1B(N_3)_3$ and Their Corresponding Barrier and Reaction Energies (in kcal·mol$^{-1}$) Calculated at Various Levels**

| | reaction | barrier height | | reaction energy | |
|---|---|---|---|---|---|
| | | CCSD(t) | B3LYP | CCSD(t) | B3LYP |
| | (1) $^1B(N_3)_3 \rightarrow {}^1BN_7 + {}^1N_2$ | | | | |
| 1 | $^1B(N_3)_3 \rightarrow {}^1NB(N_3)_2 + {}^1N_2$ | 46.6 | 49.5 | 41.8 | 42.1 |
| | (2) $^1BN_7 \rightarrow {}^1BN_5 + {}^1N_2$ | | | | |
| 2 | $^1NB(N_3)_2 \rightarrow$ *cyc*-$^1N_3BN_2 + {}^1N_2$ | −1.7 | 1.3 | −77.3 | −65.7 |
| 3 | $^1NB(N_3)_2 \rightarrow {}^1N_3BN_4$ | 1.4 | 2.2 | 1.8 | −16.0 |
| 4 | $^1N_3BN_4 \rightarrow {}^1NBN_4 + {}^1N_2$ | 13.1 | 31.5 | −8.5 | 17.9 |
| 5 | $^1N_3BN_4 \rightarrow {}^1N_3BN_2 + {}^1N_2$ | −1.0 | 13.0 | −59.0 | −25.1 |
| | (3) $^1BN_5 \rightarrow {}^1BN_3 + {}^1N_2$ | | | | |
| 6 | *cyc*-$^1N_3BN_2 \rightarrow$ *cyc*-$^1NBN_2 + N_2$ | 23.2 | 24.1 | −3.9 | 6.1 |
| 7 | *cyc*-$^1N_3BN_2 \rightarrow {}^1BNNN + N_2$ | 34.6 | 39.9 | 1.1 | 8.0 |
| 8 | $^1NBN_4 \rightarrow {}^1NBNN + N_2$ | −0.1 | 0.5 | −103.1 | −91.9 |
| 9 | $^1N_3BN_2 \rightarrow {}^1BNNN + N_2$ | −3.7 | −4.8 | −19.0 | −16.6 |
| 10 | $^1N_3BN_2 \rightarrow {}^1NBNN + N_2$ | 16.7 | 5.6 | −52.6 | −48.9 |
| | (4) $^1BN_3 \rightarrow {}^1BN + {}^1N_2$ | | | | |
| 11 | *cyc*-$^1NBN_2 \rightarrow {}^1NBNN$ | 12.1 | 11.0 | −28.6 | −30.4 |
| 12 | *cyc*-$^1NBN_2 \rightarrow {}^1BNNN$ | 32.6 | 32.8 | 5.0 | 1.9 |
| 13 | $^1BNNN \rightarrow {}^1NBNN$ | 26.8 | 25.3 | −33.6 | −32.3 |
| 14 | $^1BNNN \rightarrow {}^1BN + {}^1N_2$ | 18.5 | 48.2 | 7.2 | 33.0 |

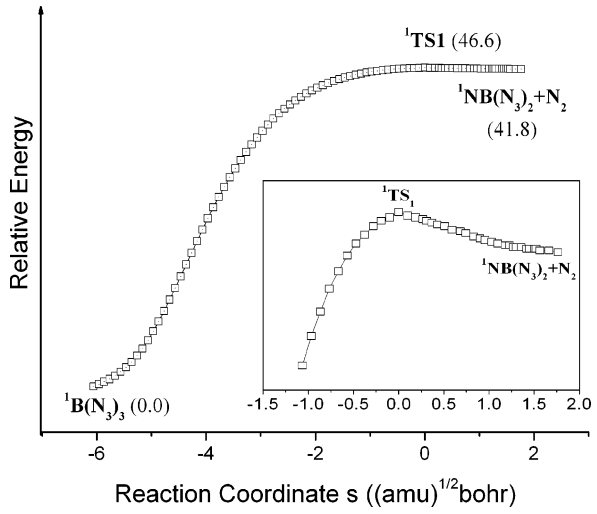


**Figure 3.** Reaction path of $^1B(N_3)_3 \rightarrow {}^1NB(N_3)_2 + {}^1N_2$ (reaction 1). The insert shows an enlargement of the IRC curve from $s = -1.0$ to 2.0.

Table 3) for $^1BN_5 \rightarrow {}^1BN_3 + {}^1N_2$ in which three isomer of $^1BN_3$, *cyc*-$^1NBN_2$, $^1$BNNN, and $^1$NBNN, are produced.

*cyc-$^1N_3BN_2 \rightarrow$ cyc-$^1NBN_2 + {}^1N_2$ (Reaction 6) and cyc-$^1N_3BN_2 \rightarrow {}^1BNNN + {}^1N_2$ (Reaction 7).* As the most stable isomer of $BN_5$, *cyc*-$^1N_3BN_2$ could decompose into *cyc*-$^1NBN_2$ or angular $^1$BNNN via transition states $^1$TS3a or $^1$TS3b, respectively. Both processes are slightly exothermic but with evident barriers: reaction 6 leading to *cyc*-$^1NBN_2$ has a barrier height of 23.2 kcal·mol$^{-1}$, and for reaction 7 34.6 kcal·mol$^{-1}$ of energy is needed to activate the B−N4 and B−N7 bonds. Therefore, the latter process may be of less importance in the decomposition of *cyc*-$^1N_3BN_2$.

*$^1NBN_4 \rightarrow {}^1NBNN + {}^1N_2$ (Reaction 8).* Decomposition of $^1NBN_4$ via transition state $^1$TS3c leads to $^1$NBNN, which is the most stable one among the isomers of $^1BN_3$. This process is strongly exothermic with more than 103.1 kcal·mol$^{-1}$ of heat liberating; moreover, it occurs easily because the activation energy is only 0.5 kcal·mol$^{-1}$ at the B3LYP/6-311++G(3df) level.

*$^1N_3BN_2 \rightarrow {}^1BNNN + {}^1N_2$ (Reaction 9) and $^1N_3BN_2 \rightarrow {}^1NBNN + {}^1N_2$ (Reaction 10).* $^1N_3BN_2$ has two potential decomposition channels: reaction 9 via $^1$TS3d leading to angular $^1$BNNN is a barrierless process, while reaction 10 via $^1$TS3d producing linear $^1$NBNN molecule has a barrier height of 16.7 kcal·mol$^{-1}$. However, the latter process is more exothermic than the former.

In step 3, decomposition of three $^1BN_5$ isomers leads to three $^1BN_3$ isomers along five channels. All reactions are exothermic. Among the products $^1$NBNN might be the dominant one because the channels generating $^1$NBNN have relatively low barrier heights and are mostly exothermic reactions.

The final step corresponds to formation of $^1$BN from $^1BN_3$. Four reactions are discussed in this step including isomerization of $^1BN_3$ and its decomposition processes (reactions 11−14, Table 3).

It is known from the above discussion that each of the three isomers of $^1BN_3$ could be produced via different channels. However, in the FTIR characterization of the photolysis products of $B(N_3)_3$ by Gilbert and co-workers they reported linear NBNN as the only intermediate that could be observed.[14] Moreover, in 1993, Martin et al. also found NBNN ($^1\Sigma^+$) as the only isomer of $BN_3$ in the products generated by boron and nitrogen atoms.[34] These facts imply there might be isomerization processes by which the cyclic and angular isomers could rearrange to the most stable one. Luckily, this prediction was supported by our calculation, three isomerization processes were found, including the following. (1) *cyc*-$^1NBN_2 \rightarrow {}^1$NBNN (reaction 11): the energy barrier of this process is about 12.1 kcal·mol$^{-1}$; therefore, the less stable *cyc*-$^1NBN_2$ tends to isomerize to $^1$NBNN with an energy release about 28.6 kcal·mol$^{-1}$. (2) *cyc*-$^1NBN_2 \rightarrow {}^1$BNNN (reaction 12): in addition, the cyclic isomer *cyc*-$^1NBN_2$ could rearrange to angular $^1$BNNN. The transition state ($^1$TS4b) and product are less stable than *cyc*-$^1NBN_2$ by 32.6 and 5.0 kcal·mol$^{-1}$, respectively. (3) $^1$BNNN $\rightarrow {}^1$NBNN (reaction 13): moreover, $^1$BNNN could also isomerize into linear $^1$NBNN. The barrier height and heat of reaction for this process are 26.8 and −33.6 kcal·mol$^{-1}$, respectively. Because the activation energies for these processes are about or less than 30 kcal·mol$^{-1}$, the heats released from the previous steps should be adequate for counteracting these barriers, especially when the reaction occurs under mild heating or UV light irradiation, which might be the reason why only linear NBNN was observed in previous experiments.

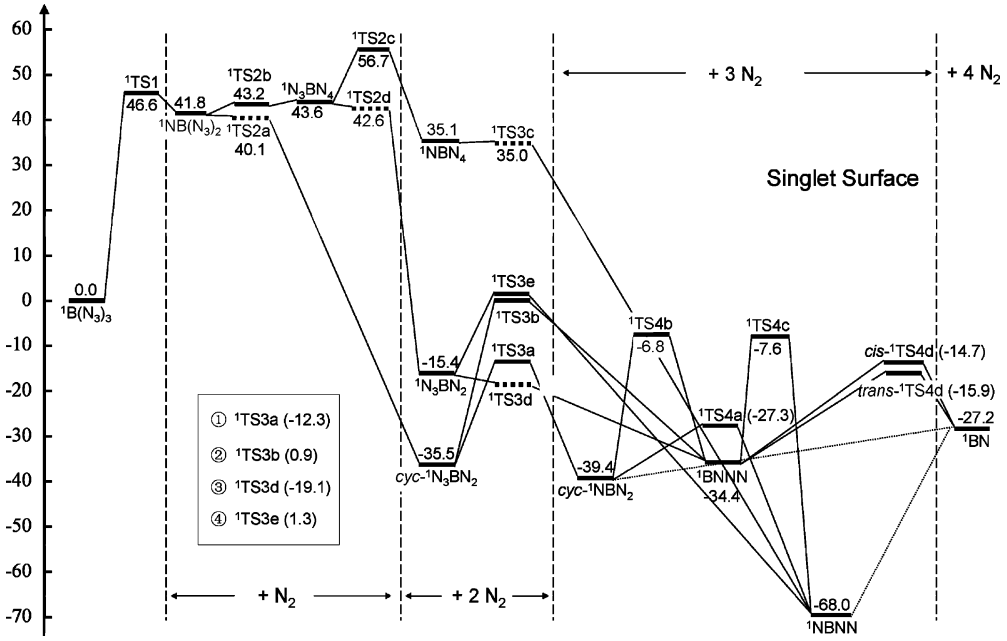


**Figure 4.** Schematic profiles of the singlet potential-energy surface for the $^1B(N_3)_3 \rightarrow {}^1BN + 4{}^1N_2$ reaction (relative energies are in kcal·mol$^{-1}$).

*$^1BNNN \rightarrow {}^1BN + {}^1N_2$ (reaction 14)*. In this step only the transition state $^1$TS4d corresponding to the decomposition of $^1$BNNN was located; for *cyc*-$^1NBN_2$ and $^1$NBNN, although great effort has being made, we still failed to find any transition states regarding their decomposition processes. They might rearrange into $^1$BNNN, then decompose or dissociate via barrierless processes. The only decomposition channel found for $^1$BNNN is endothermic; the products $^1BN + {}^1N_2$ are less stable than the reactant by 7.2 kcal·mol$^{-1}$, and the barrier for this process is 18.5 kcal·mol$^{-1}$. Compared with the relative energies of $^1BN + {}^1N_2$, $^1$NBNN has a reasonable thermodynamical stability and might be the dominant product during the singlet decomposition of $^1B(N_3)_3$ at room temperature. In other words, if $^1B(N_3)_3$ was employed as a precursor to produce BN film, a small amount of energy would be needed to overcome the barrier for the final step.

**Summary of the Singlet Mechanism.** The schematic energy profiles for the singlet reaction $^1B(N_3)_3 \rightarrow {}^1BN + 4{}^1N_2$ is presented in Figure 4. In summary, the singlet unimolecular reaction of $B(N_3)_3$ obeys a sequential mechanism. The total reaction surface is complicated, in which the favorable path might be $^1B(N_3)_3 \rightarrow {}^1NB(N_3)_2 \rightarrow$ *cyc*-$^1N_3BN_2 \rightarrow$ *cyc*-$^1NBN_2 \rightarrow {}^1$NBNN; most of other product channels should not be neglected because of their low-to-moderate activation energies, especially when a small amount of energy was input into the reacting system. The rate-determining step is the first step: $^1B(N_3)_3 \rightarrow {}^1BN_7 + {}^1N_2$, which corresponds to cleavage of the first azide bond in $^1B(N_3)_3$. The energy released from the second step of the reaction is adequate to counteract the following barriers; therefore, once the reaction is activated, it will occur spontaneously with $^1$NBNN as the dominant product at room temperature, in contrast to $^1$BN being the final product at higher temperature.

**2. Triplet Reaction Mechanism.** The triplet decomposition of $B(N_3)_3$, with final products $^3$BN and ground state $^1N_2$, is denoted $^3B(N_3)_3 \rightarrow {}^3BN + 4{}^1N_2$. Compared with the singlet reaction, this process is slightly less complicated. In all there are 11 elementary reactions and 21 stationary points on the reaction surface. The elementary reactions classified in four steps, as well as their barrier heights and heats of decomposition, are shown in Table 4.

**TABLE 4: Reactions Involved in the Triplet Decomposition Pathway of $^3B(N_3)_3$ and Their Corresponding Barrier and Reaction Energies (in kcal·mol$^{-1}$) Calculated at Various Levels**

| | | barrier height | | reaction energy | |
|---|---|---|---|---|---|
| | reaction | CCSD(t) | B3LYP | CCSD(t) | B3LYP |
| | (1) $^3B(N_3)_3 \rightarrow {}^3BN_7 + {}^1N_2$ | | | | |
| 15 | $^3B(N_3)_3 \rightarrow {}^3NB(N_3)_2 + {}^1N_2$ | 0.3 | 1.3 | −37.6 | −29.5 |
| | (2) $^3BN_7 \rightarrow {}^3BN_5 + {}^1N_2$ | | | | |
| 16 | $^3NB(N_3)_2 \rightarrow$ *cyc*-$^3N_3BN_2 + {}^1N_2$ | 60.6 | 50.1 | −14.6 | −16.1 |
| | (3) $^3BN_5 \rightarrow {}^3BN_3 + {}^1N_2$ | | | | |
| 17 | *cyc*-$^3N_3BN_2 \rightarrow {}^3N_3BN_2$ | 4.3 | 2.6 | −20.2 | −26.7 |
| 18 | *cyc*-$^3N_3BN_2 \rightarrow {}^3N_3NBN$ | 46.8 | 61.7 | 44.7 | 46.1 |
| 19 | *cyc*-$^3N_3BN_2 \rightarrow$ *cyc*-$^3NBN_2 + {}^1N_2$ | 7.5 | 8.0 | −28.0 | −17.2 |
| 20 | $^3N_3BN_2 \rightarrow {}^3NBNN + {}^1N_2$ | 15.1 | 35.0 | −12.4 | −7.7 |
| 21 | $^3N_3NBN \rightarrow$ *cyc*-$^3NBN_2 + {}^1N_2$ | 2.5 | 3.3 | −72.7 | −63.3 |
| | (4) $^1BN_3 \rightarrow {}^1BN + {}^1N_2$ | | | | |
| 22 | *cyc*-$^3NBN_2 \rightarrow {}^3NBNN$ | 8.4 | 8.4 | −4.6 | −17.2 |
| 23 | $^3NBNN \rightarrow {}^3BNNN$ | 50.7 | 63.4 | 25.0 | 36.6 |
| 24 | $^3NBNN \rightarrow {}^3BN + {}^1N_2$ | 2.2 | 60.2 | 3.4 | 47.8 |
| 25 | $^3BNNN \rightarrow {}^3BN + {}^1N_2$ | 0.2 | 1.5 | −21.6 | 11.2 |

Unlike its singlet counterpart with $C_{3h}$ symmetry, $^3B(N_3)_3$ does not show any symmetric elements (Figure 2). In $^3B(N_3)_3$, two azide groups are almost in-plane, while the last one was folded with a N7−N8−N9 angle of 122.9°; in addition, N8 moves out of the molecular plane. The energy difference between the singlet ground state and the lowest triplet state is 60.4 kcal·mol$^{-1}$, which is significantly lower than the corresponding value (143.5 kcal·mol$^{-1}$)[35] between the $X^1\Sigma_g^+$ and $A^3\Sigma_u^+$ states of $N_2$; therefore, the singlet $^1B(N_3)_3$ could be excited to the triplet state via collision with metastable $N_2$. This result is in good agreement with the experimental findings reported by Coombe et al.[12]

In the first step the transition state $^3$TS1 of $^3B(N_3)_3 \rightarrow {}^3NB(N_3)_2 + {}^1N_2$ (reaction 15) shows slight geometric difference with the reactant in which only the breaking N7−N8 bond weakens slightly. It is seen from Figure 5 that the energy barrier for this step is rather low (0.3 kcal·mol$^{-1}$), and the products are −37.6

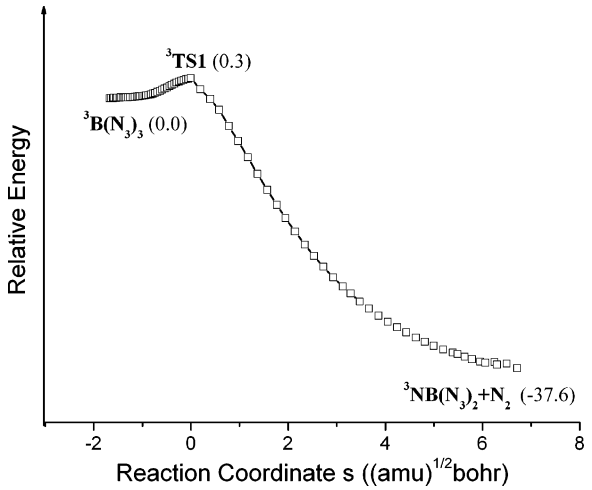


**Figure 5.** Reaction path of $^3B(N_3)_3 \rightarrow {}^3NB(N_3)_2 + {}^1N_2$ (reaction 15).

kcal·mol$^{-1}$ lower in energy than the reactant, suggesting once $B(N_3)_3$ is excited to its thermodynamically unstable triplet state, it could instantly dissociate into $^3NB(N_3)_2$ and $^1N_2$.

The second step corresponds to decomposition of $^3NB(N_3)_2$, $^3NB(N_3)_2 \rightarrow$ *cyc*-$^3N_3BN_2 + {}^1N_2$ (reaction 16). Contrary to its singlet counterparts who have a torsional azide group, $^3NB(N_3)_2$ shows a planar structure (in the singlet surface of $NB(N_3)_2$, this planar geometry is tested to be the flipping transition state between two torsional conformers). More interestingly, $^3NB(N_3)_2$ is 16.3 kcal·mol$^{-1}$ more stable than the singlet one, indicating that $NB(N_3)_2$ has an uncommon triplet ground state. The transition state $^3$TS2 for decomposition reaction 16 has $C_1$ symmetry in which N5−N6 moves out of the molecular plane. Therefore, the energy of $^3$TS2 increases significantly to 60.6 kcal·mol$^{-1}$ due to destruction of the planar geometry in $^3NB(N_3)_2$. In fact, this barrier is difficult to counteract, which makes step 2 the rate-determining step during the overall triplet reaction. From Figure 6 it is seen that $^3NB(N_3)_2$ is located in a deep well on the decomposition surface of $^3B(N_3)_3$. These findings are interesting because they imply that $^3NB(N_3)_2$ might not prefer to decompose on the triplet surface; instead, there might be alternative paths, such as intersystem crossing by which it could transfer into the energetically flexible singlet surface. It is beyond the ability of density functional theory and will be discussed in the section 3.

The product of step 2, *cyc*-$^3N_3BN_2$, is involved in various reaction processes (reactions 17−21, in Table 4), including isomerizing to $^3N_3BN_2$ and $^3N_3NBN$ and decomposing into $^3BN_3$ and $^1N_2$ as well $^3N_3BN_2$ and $^3N_3NBN$ could also decompose into smaller $BN_3$ fragments via alternative channels.

*cyc*-$^3N_3BN_2$ could rearrange into open-chain $^3N_3BN_2$ and $^3N_3NBN$ via reactions 17 and 18, respectively. The former channel via $^3$TS3b has a rather low barrier (4.3 kcal·mol$^{-1}$), and meanwhile the product $^3N_3BN_2$ lies under *cyc*-$^3N_3BN_2$ and $^3N_3NBN$ by 20.2 and 64.9 kcal·mol$^{-1}$, respectively. Therefore, the rearrangement process occurs easily. The latter channel (reaction 18), which involves cleavage of the N4−N7 bond and migration of N4 atom, has a significant barrier as well as energy unfavorable products, indicating the isomerization process *cyc*-$^3N_3BN_2 \rightarrow {}^3N_3NBN$ and the consequent decomposition of $^3N_3NBN$ (reaction 21) are negligible; therefore, these processes will not be further discussed.

Both *cyc*-$^3N_3BN_2$ and $^3N_3BN_2$ will be involved in a further decomposition process to form $^3BN_3$ and $N_2$ via reactions 19 and 20, respectively. Both are exothermic with low barriers. The former channel with a barrier height of 7.5 kcal·mol$^{-1}$ leads to *cyc*-$^3NBN_2$, which is less stable than the global minimum $^3$NBNN by 4.6 kcal·mol$^{-1}$. The barrier height for decomposition of $^3N_3BN_2$, 15.1 kcal·mol$^{-1}$, is also moderate. As a result, in step 3 of the triplet reaction the decomposition of *cyc*-$^3N_3BN_2$ via two energy favorable channels leads to *cyc*-$^3NBN_2$ and $^3$NBNN. The low barrier of both channels is easily counteracted by the energy released from the previous step.

In the final step isomerization processes among three isomers of $^3BN_3$ are discussed. *cyc*-$^3NBN_2$ isomerizes readily to $^3$NBNN (reaction 22) with a low barrier of 8.4 kcal·mol$^{-1}$, while the isomerization from $^3$NBNN to $^3$BNNN (reaction 23) has a significant barrier of 50.7 kcal·mol$^{-1}$. In addition, the latter is strongly endothermic. Thus, both the rearrangement process $^3NBNN \rightarrow {}^3BNNN$ (reaction 23) and the decomposition of $^3$BNNN (reaction 25) might play minor roles in the overall surface.

In contrast to the significant activation barrier in the decomposition of $^1$NBNN, decomposition of $^3$NBNN (reaction 24) has by far the lowest activation energy (0.2 kcal·mol$^{-1}$), so that it could decompose instantly to $^3BN$ and $N_2$. The final product $^3BN$ lies above the singlet $^1BN$ by 8.5 kcal·mol$^{-1}$, differing from a previous report[36] in which $^3BN$ was predicted as the ground state and the singlet BN ($a^1\Sigma^+$) was only 381 ± 100 cm$^{-1}$ less stable than the triplet one.

**Summary of the Triplet Mechanism.** The schematic energy profiles for the triplet reaction $^3B(N_3)_3 \rightarrow {}^3BN + 4{}^1N_2$ are presented in Figure 6. In summary, the ground-state $B(N_3)_3$ could be excited to its triplet state via collision with triplet $N_2$, and then $^3B(N_3)_3$ decomposes via a triplet path. Similar to the singlet pathway, decomposition of $^3B(N_3)_3$ is in a four-step sequential manner. Decomposition of $^3BN_7$ to form $^3BN_5$ is predicted as the rate-determining step during the overall reaction; if this barrier is overcome, the subsequent decomposition processes could easily occur with final product $^3BN$. It is also mentioned that the triplet $^3NB(N_3)_2$ is located in a potential well of the reaction surface; in addition, it is more stable than its singlet counterpart, so besides direct decomposition, there might be alternative paths by which $^3NB(N_3)_2$ may transfer to the singlet reaction pathway.

**3. Possible Mechanism for BN Film Generation.** The above-mentioned calculation results suggest $B(N_3)_3$ could decompose on either its singlet or its triplet surface. Generally, the singlet mechanism should be responsible for the thermal decomposition of boron triazide, while for the triplet reaction, which should play an important role in $B(N_3)_3$ decomposing under photolysis or collision with excited $N_2$ stream, it is hard to be an effective channel to form final products BN because of the significant barrier during the decomposition of $^3NB(N_3)_2$ (reaction 16). Therefore, to interpret the formation of BN film, neither the singlet nor the triplet mechanism is sufficient. That is, the relation between them must be carefully examined at a multiconfiguration SCF level of theory.

As mentioned in section 2, the triplet $^3NB(N_3)_2$ lies below its singlet counterpart, in contrast to other boron nitrides which have a singlet ground state. Therefore, intersystem crossing between the singlet reaction surface and the triplet one should occur. Indeed, it was located at the CAS(6,4)/6-31G(d) level of theory, with an energy difference of less than 0.02 kcal·mol$^{-1}$ between the two states. The optimization geometries of $^3NB(N_3)_2$ and $^1NB(N_3)_2$ and ISC between them are shown in Figure 7. From Figure 7 it is seen that the geometries of $^3NB(N_3)_2$ and $^1NB(N_3)_2$ are consistent with those of B3LYP optimization, with the former being 9.3 kcal·mol$^{-1}$ more stable than the latter. The ISC, which is structurally the average of the singlet $NB(N_3)_2$

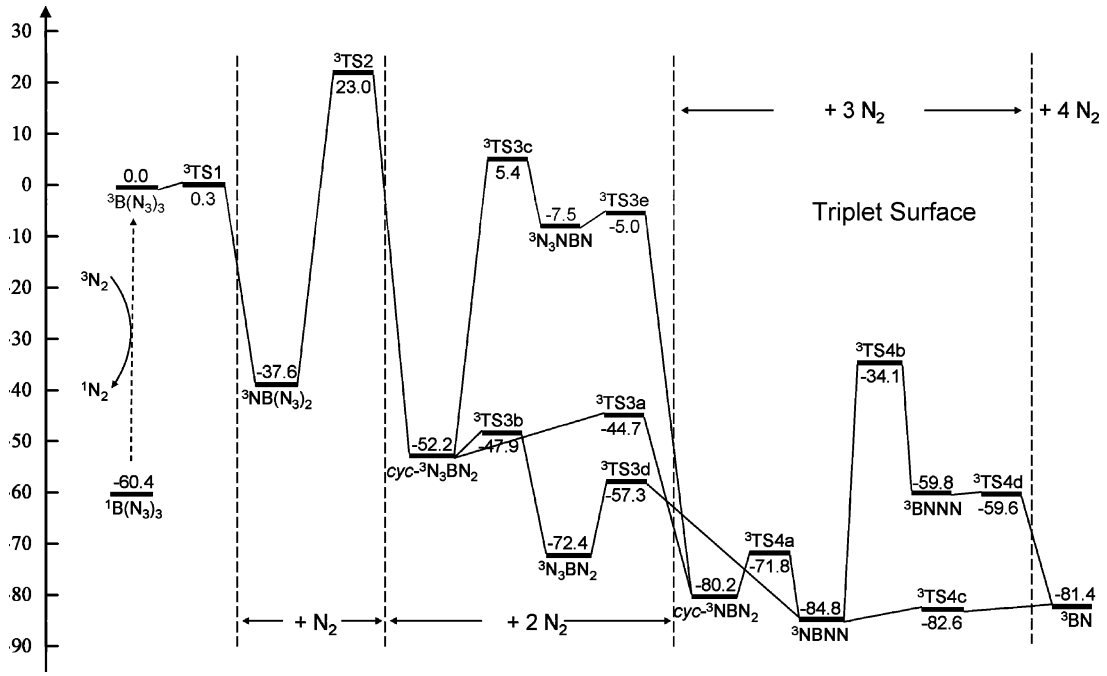


**Figure 6.** Schematic profiles of the singlet potential-energy surface for the $^3B(N_3)_3 \rightarrow {}^3BN + 4\,{}^1N_2$ reaction (relative energies are in kcal·mol$^{-1}$).

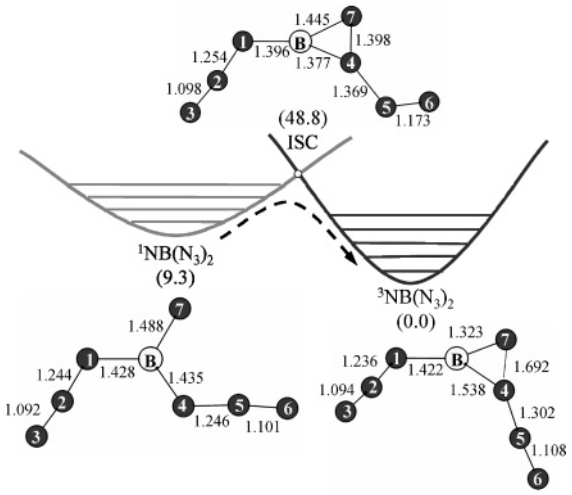


**Figure 7.** CASSCF/6-31G(d)-optimized geometries and schematic profile for the ISC between the singlet and triplet states of $BN_7$.

and triplet one, lies 48.8 kcal·mol$^{-1}$ above the triplet ground state but is still under the transition state $^3$TS2 by 11.8 kcal·mol$^{-1}$.

On the basis of these results it is possible that the triplet $^3NB(N_3)_2$ transfers into its singlet surface via the ISC between the two states then decomposes on the singlet surface; accordingly, the significant barrier during $^3NB(N_3)_2 \rightarrow$ *cyc*-$^3N_3BN_2 + {}^1N_2$ (reaction 16) is avoided. Therefore, under irradiation with UV light or collision with excited $N_2$ stream, the mechanism for generating BN film via $B(N_3)_3$ precursor is suggested as follows: $B(N_3)_3$ is first excited from its singlet ground state to the triplet state and then readily decomposes into $^3NB(N_3)_2$; $^3NB(N_3)_2$ could decompose on the triplet surface to form final product BN; on the other hand, it could also transfer to its singlet surface via ISC (Figure 7) and consequently dissociate to produce BN film. This suggestion might be helpful in understanding the possible mechanism for BN film generation.

**Acknowledgment.** This project was supported by the National Natural Science Foundation of China (NSFC-20573032) and Natural Science Foundation of Hebei Province (B2004000147, B2006000137).

**Supporting Information Available:** Vibrational frequencies for reactant, intermediates, transition states, and products of the reactions; IRC path for all reactions (pdf). This material is available free of charge via the Internet at http://pubs.acs.org.

## References and Notes

(1) Wibera, E.; Michaud, H. Z. *Naturforsch.* **1954**, *96*, 497.
(2) Paetzold, P. I. *Adv. Inorg. Chem.* **1987**, *31*, 123.
(3) Müller, J.; Paetzold, P. I. *Heteroat. Chem.* **1990**, *1*, 461.
(4) Fraenk, W.; Habereder, T.; Hammerl, A.; Klapötke, T. M.; Krumm, B.; Mayer, P.; Nöth, H.; Warchhold, M. *Inorg. Chem.* **2001**, *40*, 1334.
(5) Mulinax, R. L.; Okin, G. S.; Coombe, R. D. *J. Phys. Chem.* **1995**, *99*, 6294.
(6) *Synthesis and Properties of Boron Nitride*; Pouch, J., Alterovitz, A., Eds.; Trans Tech: Aedermannsdorf, Switzerland, 1990; Materials Science Forum, Vol. 54/55.
(7) Iijima, S. *Nature* **1991**, *354*, 56.
(8) Han, W.-Q.; Fan, S.-S.; Li, Q.-Q.; Hu, Y.-D.*Science* **1997**, *277*, 1287.
(9) Arya, S. P. S.; D'Amico, A. *Thin Solid Films* **1988**, *157*, 267.
(10) Vel, L.; Demazeau, G.; Etourneau, J. *Mater. Sci. Eng.* **1991**, *B10*, 149.
(11) Moriyoshi, Y.; Komatsu, S.; Ishigaki, T. *Key Eng. Mater.* **1995**, *111/112*, 267.
(12) Hobbs, K. R.; Coombe, R. D. *J. Appl. Phys.* **2000**, *87*, 4586.
(13) Hobbs, K. R.; Coombe, R. D. *Thin Solid Films* **2002**, *402*, 162.
(14) Al-Jihad, I. A.; Liu, B.; Linnen, C. J.; Gilbert, J. V. *J. Phys. Chem.* **1998**, *102*, 6220.
(15) Liu, F.-Y.; Zeng, X.-Q.; Zhang, J.-P.; Meng, L.-P.; Zheng, S.-J.; Ge, M.-F.; Wang, D.-X.; Mok, D. K. W.; Chau, F.-T. *Chem. Phys. Lett.* **2006**, *419*, 213.
(16) MacDonald, M. A.; David, S. J.; Coombe, R. D. *J. Chem. Phys.* **1986**, *84*, 5513.
(17) Coombe, R. D.; Patel, D.; Pritt, A. T., Jr.; Wodarczk, F. J. *J. Chem. Phys.* **1981**, *75*, 2177.
(18) Johnson, L. A.; Sturgis, S. A.; Al-Jihad, I. A.; Liu, B.; Gilbert, J. V.*J. Phys. Chem. A* **1999**, *103*, 686.
(19) Travers, M. J.; Eldenburg, E. L.; Gilbert, J. V. *J. Phys. Chem. A* **1999**, *103*, 9661.
(20) Travers, M. J.; Gilbert, J. V. *J. Phys. Chem. A* **2000**, *104*, 3780.

(21) Arenas, J. F.; Marcos, J. I.; Otero, J. C.; Sánchez-Gálvez, A.; Soto, J. *J. Chem. Phys.* **1999**, *111*, 551.
(22) Arenas, J. F.; Marcos, J. I.; López-Tocón, I.; Otero, J. C.; Soto, J. *J. Chem. Phys.* **2000**, *113*, 2282.
(23) Netzloff, H. M.; Gordon, M. S. *J. Phys. Chem. A* **2003**, *107*, 6638.
(24) Fan, Y.; Hall, M. B. *Chem. Eur. J.* **2004**, *10*, 1805.
(25) Becke, A. D. *J. Chem. Phys.* **1992**, *96*, 2155.
(26) Becke, A. D. *J. Chem. Phys.* **1993**, *98*, 5648.
(27) Gonzalez, C.; Schlegel, H. B. *J. Chem. Phys.* **1989**, *90*, 2514.
(28) Bartlett, R. J.; Purvis, G. D. *Int. J. Quantum Chem.* **1978**, *14*, 516.
(29) Dunning, T. H. *J. Chem. Phys.* **1989**, *90*, 1007.
(30) Frisch, M. J.; Ragazos, I. N.; Robb, M. A.; Schlegel, H. B. *Chem. Phys. Lett.* **1992**, *189*, 524.
(31) Frisch, M. J.; Trucks, H. B. Schlegel, G. W.; Scuseria, G. E.; Robb, M. A.; Cheeseman, J. R.; Zakrzewski, V. G.; Montgomery, J. A.; Stratmann, R. E.; Burant, J. C.; Dapprich, S.; Millam, J. M.; Daniels, A. D.; Kudin, K. N.; Strain, M. C.; Farkas, O.; Tomasi, J.; Barone, V.; Cossi, M.; Cammi, R.; Mennucci, B.; Pomelli, C.; Adamo, C.; Clifford, S.; Ochterski, J.; Petersson, G. A.; Ayala, P. Y.; Cui, Q.; Morokuma, K.; Malick, D. K.; Rabuck, A. D.; Raghavachari, K.; Foresman, J. B.; Cioslowski, J.; Ortiz, J. V.; Baboul, A. G.; Stefanov, B. B.; Liu, G.; Liashenko, A.; Piskorz, P.; Komaromi, I.; Gomperts, R.; Martin, R. L.; Fox, D. J.; Keith, T.; Al-Laham, M. A.; Peng, C. Y.; Nanayakkara, A.; Gonzalez, C.; Challacombe, M.; Gill, P. M. W.; Johnson, B.; Chen, W.; Wong, M. W.; Andres, J. L.; Gonzalez, C.; Head-Gordon, M.; Replogle, E. S.; Pople, J. A. *Gaussian 98*; Gaussian, Inc.: Pittsburgh, PA, 1998.
(32) Hammerl, A.; Klapötke, T. M.; Schwerdtfeger, P. *Chem. Eur. J.* **2003**, *9*, 5511.
(33) Zeng, Y.-L.; Sun, Q.; Meng, L.-P.; Zheng, S.-J.; Wang, D.-X. *Chem. Phys. Lett.* **2004**, *390*, 362.
(34) Andrews, L.; Hassanzadeh, P.; Burkholder, T. R.; Martin, J. M. L. *J. Chem. Phys.* **1993**, *98*, 922.
(35) Huber, K. P.; Herzberg, G. *Molecular Spectra and Molecular Structure*; Van Nostrand Reinhold: New York, 1979.
(36) Martin, J. M. L.; Lee, T. J.; Scuseria, G. E.; Tayplor, P. R. *J. Chem. Phys.* **1992**, *97*, 6549.